Periodic Cages

Mircea V. Diudea,*,† Csaba L. Nagy,† Ioan Silaghi-Dumitrescu,† Ante Graovac,‡,§ Dušanka Janežič,|| and Dražen Vikić-Topić‡

Faculty of Chemistry and Chemical Engineering, "Babes-Bolyai" University, 400084 Cluj, Romania, The R. Bošković Institute, P.O. Box 180, HR-10002 Zagreb, Croatia, Faculty of Natural Sciences, Mathematics and Education, Nikole Tesle 12, HR-21000 Split, Croatia, and National Institute of Chemistry, Hajdrihova 19, SI-1000 Ljubljana, Slovenia

Received August 24, 2004

Various cages are constructed by using three types of caps: *f*-cap (derived from spherical fullerenes by deleting zones of various size), *kf*-cap (obtainable by cutting off the polar ring, of size *k*), and *t*-cap ("tubercule"-cap). Building ways are presented, some of them being possible isomerization routes in the real chemistry of fullerenes. Periodic cages with ((5,7)3) covering are modeled, and their constitutive typing enumeration is given. Spectral data revealed some electronic periodicity in fullerene clusters. Semiempirical and strain energy calculations complete their characterization.

INTRODUCTION

Carbon allotropes with finite molecular cage structures became nowadays parts of real chemistry: they have been functionalized or inserted in supramolecular assemblies.[1−7]

A fullerene is, according to a classical definition, an all-carbon molecule consisting entirely of pentagons (exactly 12) and hexagons ($N/2-10$). Nonclassical fullerene extensions to include rings of other sizes have been considered.[8−10]

This paper presents some ways for obtaining, in silico, of various cages and their interconversion by well-known isomerization reactions. The text is organized as follows. Construction of various tubulenes is described in the Capping Nanotube section. The Periodic Cages section presents the construction of periodic ((5,7)3) nanostructures and data of their topology.

Interconversion routes among some interesting nanostructures are given in the Isomerizing Capped Nanotubes section. The Energetics and Spectral Data section gives an insight of the electronic characteristics of the discussed nanostructures, while Strain Energy Calculation completes the energetic aspects given in the previous section. Some rules of thumb, useful in the trial of the most stable structures, among thousands of topological isomers are presented in the Discussion section. A brief survey is given in Conclusions.

CAPPING NANOTUBES

Covering transformation is one of the ways in understanding chemical reactions occurring in fullerenes.[11−13] A capped nanotube we call here a tubulene. Covering is different for the caps and for the nanotube distancing the two caps. Within this paper three types of caps are discussed: (1) *f*-cap, derived from spherical fullerenes by deleting zones of various size and fitted to polyhex "armchair" (6,3)A and "zigzag" (6,3)Z nanotubes, respectively; (2) *kf*-cap, obtainable by cutting off the polar ring (of size *k*) and fitted to Z nanotubes, and (3) *t*-cap, suitable to variously covered nanotubes. When no ambiguity exists, the specification for polyhex (6,3) covering is omitted. Conversely, when a different covering pattern is needed, it has to be specified (see below). Both the cap and nanotube coverings can be changed by appropriate operations.

The *f*-Capped Tubulenes. Various caps and various junction zones could be used to construct tubulenes or oligomeric species.[14,15] The name of a cap includes the number of atoms *N*, the *a*-spiral code,[16] and the fitting tube specification, e.g., A/Z[*c*,*n*], with *c* being the number of atoms in the cross-section while *n* is the number of such sections along the tube. Note the value $n = 0$ for the tube length in a cap, e.g., $C_{36(66^65^6)-A[12,0]}$. Also note that, in two integer parameter (*k*,*l*) notation,[17] the armchair (single-walled) nanotube SWNT is (*c*/2, *c*/2) while the zigzag one is (*c*/2,0). Figure 1 illustrates *f*-tubulenes containing A and Z nanotubes, respectively.

The name of a tubulene is made as of the cap, taking now $n \geq 0$ and adding the tessellation of the zone between the two caps, e.g., $C_{168(6(56)^3(665)^3)-Z[18,5]}$. According to the fitted nanotube, these cages are called *fa*- or *fz*-tubulenes.

The *kf*-Capped Tubulenes. By cutting off the polar ring *k* of a spherical fullerene, a "*k*-deleted fullerene *kf*-cap" is obtained. Such caps fit to Z nanotubes. Figure 2 illustrates two peanut-shaped *kf*-tubulenes with different nanotubes (observe the complete description of covering) distancing the two caps, $C_{66(66^6(56)^6(65)^6-Z[12,0])}$.

The cages in Figure 3 have even shorter distancing tube (one atom and zero atom rows, respectively) between the two caps. The name of such tubulenes includes the code for the cap and distancing zone up to the second cap, if the two caps are identical, or full description, if they are different.

The *t*-Capped Tubulenes. The "tubercule"-like *t*-cap $C_{24(65^61^6-A[12,0])}$ (Figure 4), conceivable to evolve from the open end(s) of an A nanotube by adding C_2 units up to closure,[18] is a third type of cap herein discussed. The resulting

* Corresponding author e-mail: diudea@chem.ubbcluj.ro.
† "Babes-Bolyai" University.
‡ The R. Bošković Institute.
§ Nikole Tesle 12.
|| National Institute of Chemistry.

10.1021/ci049738g CCC: $30.25
Published on Web 02/12/2005

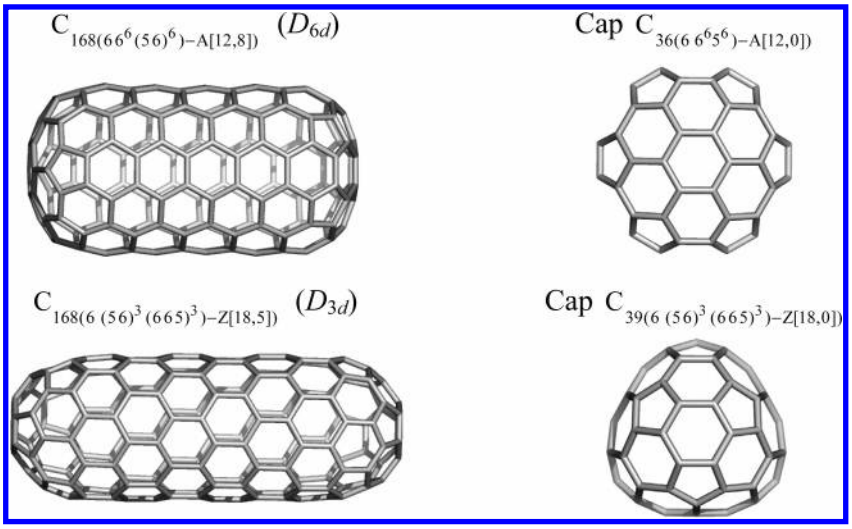

Figure 1. Examples of *fa*- and *fz*-tubulenes.

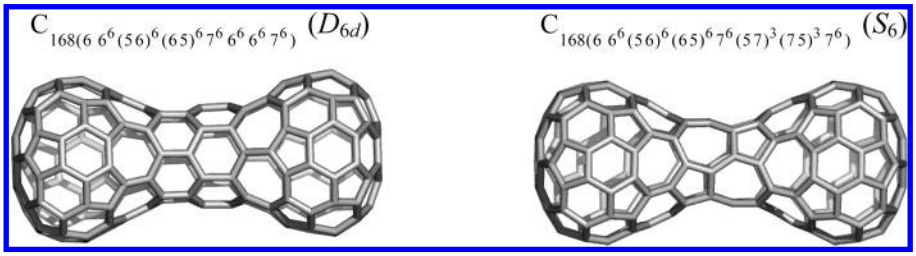

Figure 2. Peanut-shaped *kf*-tubulenes.

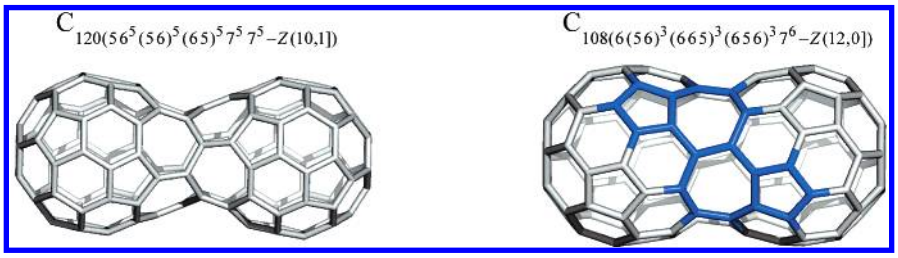

Figure 3. Peanut-shaped *kf*-tubulenes with the shortest distancing tube.

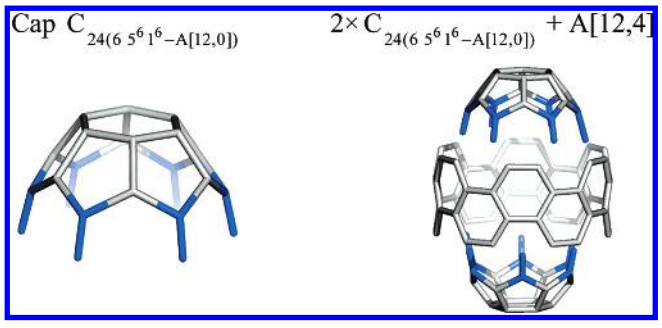

Figure 4. Capping an A nanotube by a "tubercule" *t*-cap.

ta-tubulene $C_{96(65^67^6(56)^6(65)^6-A[12,4])}(C_2)$ (see Figure 9) has the equatorial zone tessellated as in C_{60}.

A similar cap $C_{21(75^7-Z[14,0])}$ fits to a suitable phenylenic ((4,6)3)H tube[19] (Figure 5) to give a cage $C_{84(75^77^7(46)^77^75^77)}$ (Figure 10), which further rearranges to a cage decorated with only pentagons and heptagons (see below).

PERIODIC CAGES

Cutting off the polar ring of a $C_{12k(k5^k7^k5^{2k}7^k5^kk)}$ cage and identifying the boundary of two such cut-cages results in a "dimer" $C_{20k(k5^k(7^k5^{2k}7^k)^25^kk)}$ (Figure 6, $k = 7$).

In the general formula $C_{N(k5^k(7^k5^{2k}7^k)^r5^kk)}$ of these periodic cages, $N = 4k(2r + 1)$ (see Table 1), next is the spiral code, while r counts the spheroidal repeat units, $r = 2, 3, \ldots$. The coupling process can continue to give oligomers.

At moderate temperature and pressure (300 °C and 1 GPa) spherical fullerenes arrange in one-dimensional assemblies.[20] This paper suggested the existence of periodic fulleroids that we just modeled. An oligomeric cage is illustrated in Figure 7.

It is note worthy the phantasmagorical fullerene designed by Fowler and that of Dress, having 260 points, $f_5 = f_7 + 12$; $f_7 = 60{\cdot}m$; $m = 1$, and icosahedral symmetry.[21] A third cage of the same covering is constructed by the actual procedure (Figure 7).

(5,7) Periodic Cages Typing Theorem. For a periodic cage ((5,7)3) the number of faces, edges, and vertices of the various types can be counted as functions of the repeat unit r and the polar cycle size k (Table 1). Demonstration is given by construction.

ISOMERIZING CAPPED NANOTUBES

The peanut $C_{168(66^6(56)^6(65)^67^66^66^67^6)}(D_{6d})$ (Figure 2) isomerizes to the peanut $C_{168(66^6(56)^6(65)^67^6(57)^3(75)^37^6)}(S_6)$, with azulenic tiling

Figure 5. Elementary units in building all (5,7) cages.

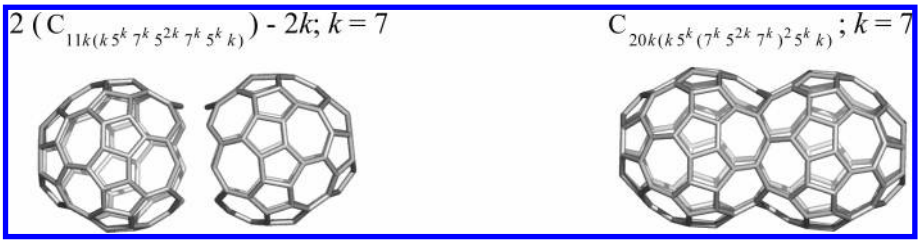

Figure 6. An in silico dimerization process.

Table 1. ((5,7)3) Periodic Cages−Net Counting[a]

formulas for $k = 5; 7$	
$f_{5k} = 2k(r + 1) + 2t_5$	(1)
$f_{7k} = 2kr + 2t_7$	(2)
$e_{5,5k} = 2k(r + 1 + t_5)$	(3)
$e_{5,7k} = 2k(3r + 2 + t_7)$	(4)
$e_{7,7k} = 2k(2r - 1)$	(5)
$v_{5,5,5k} = 2kt_5$	(6)
$v_{5,5,7k} = 2k(2r + 1 + t_7)$	(7)
$v_{5,7,7k} = 2k(r + 1)$	(8)
$v_{7,7,7k} = 2k(r - 1)$	(9)
$N_k = 4k(2r + 1)$	(10)

[a] $t_s = 1$ if $s = k$, and zero otherwise.

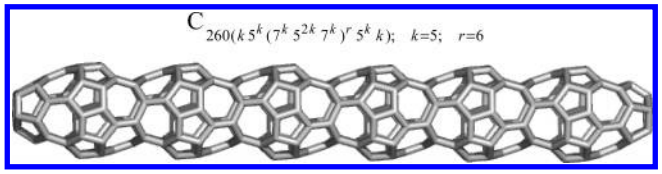

Figure 7. Diudea's C_{260} ((5,7)3) cage.

on the distancing tube by (three) Stone−Walls SW edge rotations[11] (see the necks and their geodesic projections in Figure 8). Some energetic and spectral data for the above cages are given below.

The *ta*-tubulene $C_{96(65^67^6(56)^6(65)^67^65^66)}$ (C_2) may isomerize[18] to the fullerene $C_{96(66^6(56)^6(66)^6(65)^66^66)}$($D_{6d}$) by cascade SW rotation of the marked edges. The two structures are presented in Figure 9 both as 3D objects and geodesic projections.

A similar process could transform the (4,6) pair in $C_{84(75^77^7(46)^77^75^77)}$ into the (5,5) pair in $C_{84(75^77^75^{14}7^75^77)}$ (Figure 10). The SW isomerization of cages of general formula $C_{12k(k5^k7^k5^{2k}7^k5^kk)}$ leads to the classical $C_{12k(k6^k(56)^k(65)^k6^kk)}$ fullerenes, as shown in Figure 11.

Isomerization of the peanut $C_{100(55^5(7^55^{10}7^5)^25^55)}$ (Figure 12) to the corresponding *fa*-tubulene $C_{100(56^5(56)^5-A[10,2])}$ could occur by two ways as the SW rotation process starts: (i) by the "red" bonds sharing two heptagons in the zone of joining the two repeat units and (ii) the "blue" bonds at the cap region. The stepwise process is given in Figure 12 while the corresponding energetic and spectral data will be given below.

SEMIEMPIRICAL AND STRAIN ENERGY CALCULATIONS

Semiempirical calculations have been performed on a 2x1GHz Pentium III PC by using the PM3 or MNDO Hamiltonians, in standard parametrization supplied by HyperChem (version 4.5, Hypercube, Inc.)[22] software. Structures were optimized by using the Polak−Ribier conjugate−gradient method. The energy minimization was terminated at an RMS gradient <0.01 kcal/(Å·mol) for all structures.

We calculated heat of formation HF (kcal/mol) and HOMO−LUMO gap (eV) as a rough measure of thermodynamic and kinetic stability, respectively.

Strain energy was calculated in terms of the POAV1 theory,[23−26] which defines the π-orbital axis vector is as the vector making equal angles $\theta_{\sigma\pi}$ to the three σ-bonds of the sp^2 carbon atom and a pyramidalization angle as:

$$\theta_p = \theta_{\sigma\pi} - 90° \qquad (11)$$

This angle is used for estimating the strain energy, induced by a pyramidalized carbon atom, by

$$SE = 200\cdot(\theta_p)^2 \qquad (12)$$

with θ_p being measured in radians. The difference $120 - (1/3)\sum\theta_{ij}$ gives the deviation to planarity. POAV analysis provides a reliable description of electronic structure of nonplanar conjugated molecules.

Spectral data (see Discussion) were calculated by TOPO-CLUJ 2.0 Software Package.[27]

Semiempirical data for the tubulenes in Figures 2 and 8, all having 168 atoms, are presented in Table 2.

Calculations for some ((5,7)3) periodic cages are given in Table 3. Only the dimeric $C_{140(75^7(7^75^{17}7^7)^25^77-Z(14,1))}$ (entry 4) appears to have the HF closer to C_{60} (entry 5), while the electronic structure is pseudo-closed or open (see Discussion).

Data for the isomerization process illustrated in Figure 12 are presented in Table 4. Data for the peanut cages in Figure 3 and their corresponding *f*-tubulenes (Figure 13) are given in Table 5.

DISCUSSION

Various cages and building ways have been presented above. Some of them are included in possible isomerization routes in the real chemistry of fullerenes.

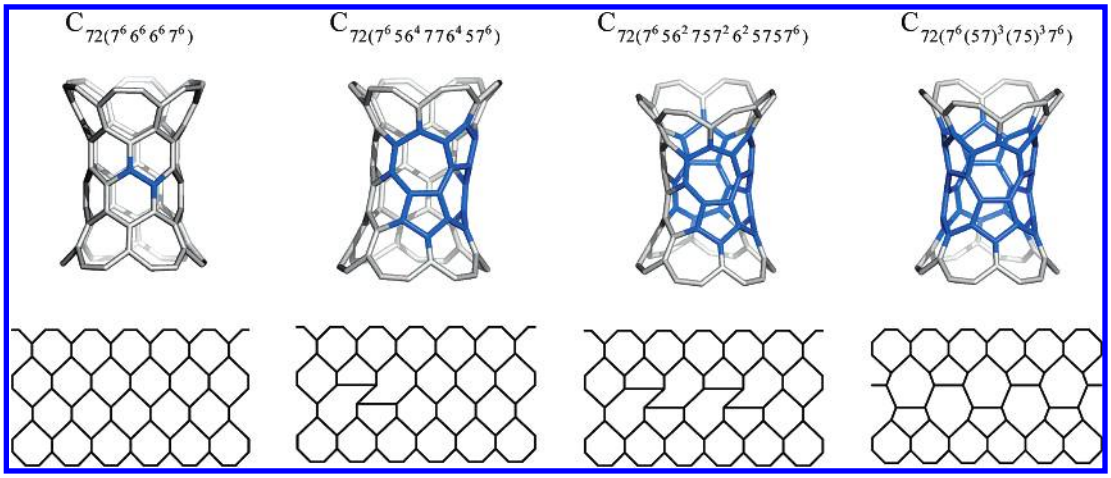

Figure 8. SW isomerization of the necks of the peanut cages from the polyhex $C_{72(7^6 6^6 6^6 7^6)}$ to azulenic $C_{72(7^6(57)^3(75)^3 7^6)}$ and their geodesic projections.

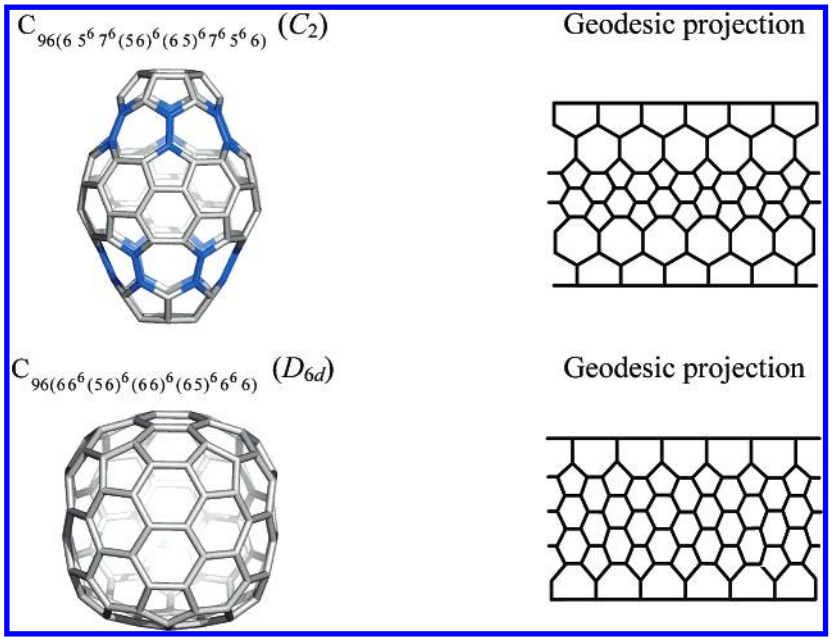

Figure 9. Quasi-spherical cages and their geodesic projections.

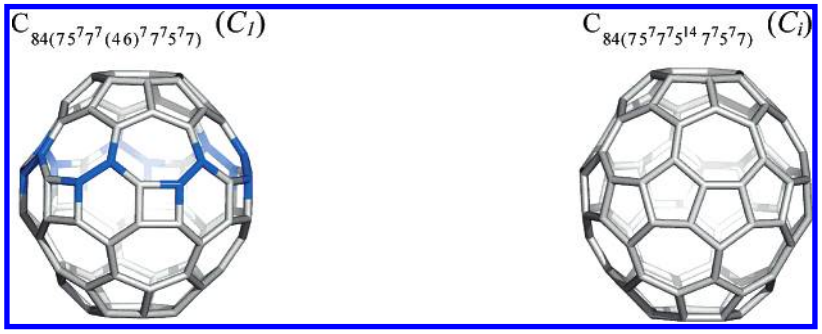

Figure 10. SW transformation rearranging pairs (4,6) to (5,5) ones.

Several cages (oligomeric structures included) showed HF values in the range of C_{60} (see Tables 3 and 5) and lower than their monomeric parents (Tables 2, 4, and 5). Cages in Tables 2 and 4 can be viewed as intermediates finally turning to the more stable, properly closed PC tubulenes.

In the Spectral Theory, at the simple π-only Hückel[28] level of theory, the energy of the ith molecular orbital $E_i = \alpha + \lambda_i\beta$ is calculated on the grounds of the adjacency matrix associated to the molecular hydrogen-depleted graph.

The π-electronic shells of neutral fullerenes are classified, function of their eigenvalue spectra, as[29−32] (i) properly closed or PC when $\lambda_{N/2} > 0 \geq \lambda_{N/2+1}$; (ii) pseudo-closed or PSC in case $\lambda_{N/2} > \lambda_{N/2+1} > 0$; (iii) meta-closed or MC with $0 \geq \lambda_{N/2} > \lambda_{N/2+1}$; and (iv) open or OP when the $N/2$th (HOMO) and $N/2 + 1$th (LUMO) molecular orbitals are degenerate, $\lambda_{N/2} = \lambda_{N/2+1}$. The band gap (in β units) is taken as the absolute value of the difference $E_{(\mathrm{HOMO})} - E_{(\mathrm{LUMO})}$.

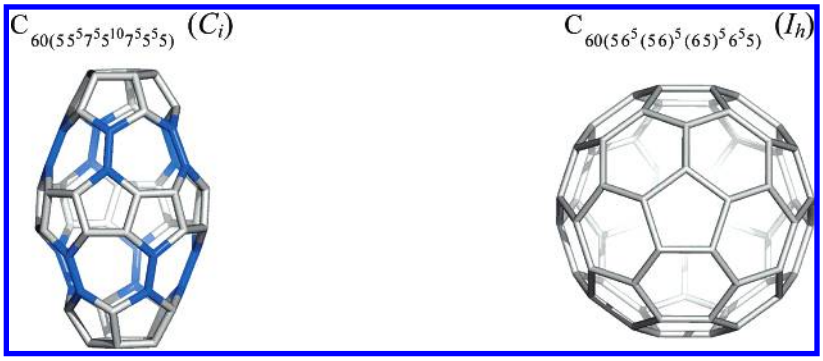

Figure 11. Isomerization of all ((5,7)3) cages leading to the classical C_{12k} fullerenes.

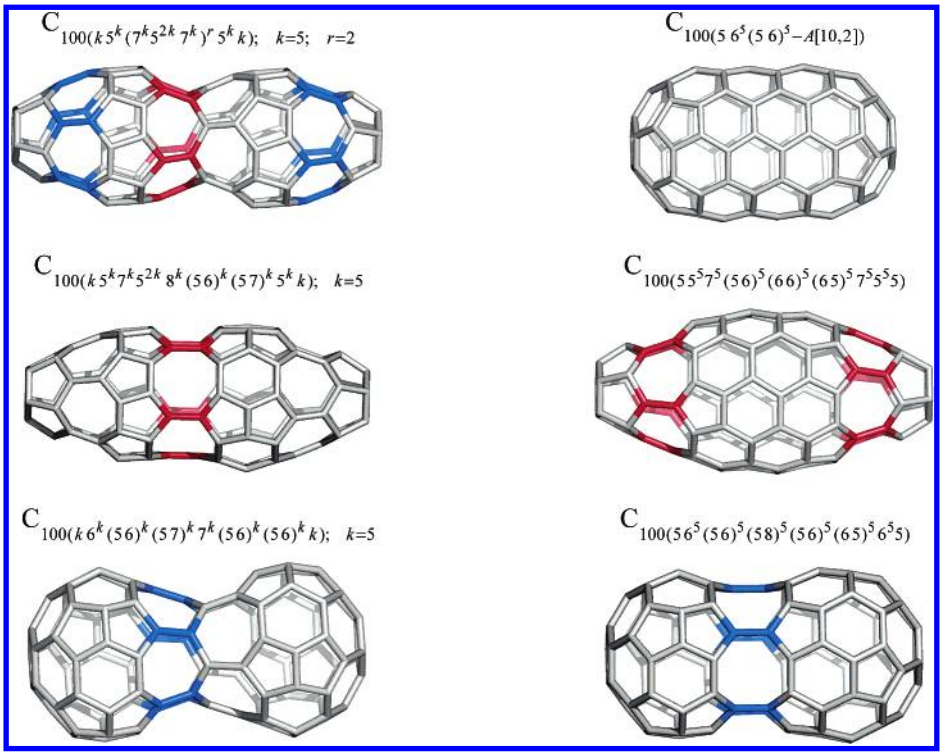

Figure 12. Isomerization of all (5,7) cages leading to classical *fa*-tubulenes.

Table 2. PM3 Data for Some A/Z Tubulenes (Figures 1, 2 and 8)

	cage	N	sym.	PM3/ (HF/atom)	PM3 gap
1	$C_{168(66^6(56)^6)-A[12,6])}$	168	D_{6d}	8.676	3.510
2	$C_{168(6(56)^3(665)^3)-Z[18,5])}$	168	D_{3d}	9.138	4.418
3	$C_{168(66^6(56)^6(65)^66^66^66^7)}$	168	D_{6d}	11.927	5.114
4	$C_{168(66^6(56)^6(65)^67^65^4776^457^6)}$	168	C_2	12.261	5.157
5	$C_{168(66^6(56)^6(65)^67^656^2757^26^25757^6)}$	168	C_2	12.452	5.194
6	$C_{168(66^6(56)^6(65)^67^6(57)^3(75)^37^6)}$	168	S_6	12.553	5.425

Systematic studies on adjacency matrix associated to the molecular hydrogen depleted graph and their eigenvalue spectra (i.e., the decreasing sequence of eigenvalues λ_i) provided some magic number rules for the stability of molecules, such as the oldest Hückel $4n + 2$ rule for aromatic rings and the more recent $60 + 6m$ ($m \neq 1$) leapfrog rule[30] LER for the properly closed fullerenes.

The most frequent case is that of the pseudo-closed shell PSC, since, in fullerenes, the number of positive eigenvalues is, in general, larger than that of the negative ones, $n_+ \geq n_-$.[31] It implies electron deficiency, so that the charge-transfer from an electron-donating partner will stabilize their π-electronic structure.

Table 3. PM3 Data for Data for Some ((5,7)3)Periodic Cages: $C_{N(k5^k(7^k5^{2k}7^k)^r5^k k-Z(2k,1))}$

	cage *N*, *k*, *r*	sym.	HF/atom	gap
		Tube Z[10,1]		
1	60, 5, 1	C_i	21.158	5.623
2	100, 5, 2	C_i	18.906	5.592
		Tube Z[14,1]		
3	84, 7, 1	C_i	16.249	4.538
4	140, 7, 2	C_i	15.828	5.114
5	C_{60}	C_i	13.512	6.596

A properly closed-shell PC represents the optimum, with all electrons in bonding orbitals and a definite gap between occupied and empty orbitals; in this case, $n_+ = n_-$. Such structures are relatively rare and satisfy the leapfrog rule (see above) and the cylinder rules, as will be detailed in the following.

Objects of the general formula $C_{N(k6^k(56)^k-A[2k,n])}$ (like $C_{168(66^6(56)^6)-A[12,6])}$, Figure 1) with *k*-fold cylindrical symmetry, obey the armchair cylinder rule[32] or ACR, which predicts closed shell at each nuclearity $N = 12k + 2k(1 + 3m)$, $m = 0, 1, 2, ...$; $k = 4-7$. In our notation, $n = 1 + 3m$, *n* being the number of cross sections separating the two caps of a

Figure 13. *f*-tubulenes of series A and Z, respectively.

Table 4. PM3 Data for an All ((5,7)3) Cage and Its Intermediates of Isomerization to the Corresponding *fa*-Tubulene

	cage	sym.	HF/atom	gap
1	$C_{100(k5^k(7^k5^{2k}7^k)^r5^k)k=5;r=2}$	C_1	18.906	5.592
2	$C_{100(k6^k(56)^k(57)^k7^k(56)^k(56)^kk)k=5}$	D_{5d}	15.146	5.546
3	$C_{100(56^5(56)^5(58)^5(56)^5(65)^56^55)}$	C_{5v}	13.966	5.770
4	$C_{100(k5^k7^k5^{2k}8^k(56)^k(57)^k5^kk)k=5}$	C_1	18.260	5.404
5	$C_{100(55^57^5(56)^5(66)^5(65)^57^55^55)}$	D_{5d}	15.205	3.849
6	$C_{100(56^5(56)^5-A[10,2])}$	D_{5d}	10.876	5.045

Table 5. MNDO and POAV1 Data for the Peanut Cages in Figure 3 and Their Corresponding *f*-Tubulenes[a]

	cage	sym.	HF/atom	gap	S/atom (kcal/mol)
1	$C_{120(56^5(56)^5)-A[10,4])}$	D_{5d}	10.697	4.943	5.198
2	$C_{120(56^5(56)^5(65)^57^57^5-Z(10,1])}$	D_{5d}	13.071	6.315	6.309
3	$C_{114(6(56)^3(665)^3-Z(18,2])}$	D_{3h}	10.909	5.288	5.178
4	$C_{108(6(56)^3(665)^3(656)^37^6-Z(12,0])}$	D_{3d}	13.549	5.030	6.503
5	C_{60}	I_h	14.479	6.569	8.257

[a] For comparison, C_{60} is included.

Table 6. Sequence in *fa*- and *fa*-Tubulenes π-Electronic Shell Type

cage/*N*	60	70	80	...	180	190	200
$C_{N(56^5(56)^5)-A[10,n])}$	LER $m=0$	ACR $m=0$	PSC		LER $m=4$	ACR $m=4$	PSC
$C_{N(55^57^5(56)^5-A[10,n])}$			TACR $m=0$		TNACR $m=3$	PSC	TACR $m=4$

nanotube. These tubulenes have a nonbonding orbital (NBO) LUMO separated by a gap from HOMO. Exceptions have been observed. The example in Figure 1 happened to have a PSC shell. Note that, in the armchair tubulene series $C_{N(k6^k(56)^k-A[2k,n])}$, LER can be written as ACR, A-LER: $N = 12k + 2k\cdot3m$, $m = 0, 1, 2, ...$; $k = 4-7$.

Objects such as $C_{96(65^67^6(56)^6(65)^67^65^66)}$ (Figure 9) belong to *ta*-tubulenes $C_{N(k5^k7^k(56)^k-A[2k,n])}$. They follow the *t*-armchair cylinder rule[17] or TACR that states the periodicity of closed shells at nuclearity $N = 8k + 2k(4 + 3m)$; $m = 0, 1, 2, ...$ Recalculated for the $C_{N(k6^k(56)^k-A[2k,n])}$ series, it can be written as $N = 12k + 2k(2 + 3m)$; $m = 0, 1, 2, ...$

In the same series, a second rule, called *tn*-armchair cylinder rule[18] or TNACR predicts closed shells (but LUMO being an NBO) at $N = 8k + 2k(11 + 3m)$; $m = 0, 1, 2, ...$ or, in the $C_{N(k6^k(56)^k-A[2k,n])}$ series, $N = 12k + 2k(3 + 3m)$; $m = 2, 3, ...$

The *ta*-tubulenes have nuclearities that interlace with those of *fa*-tubulenes and a similar periodicity of their HOMO−LUMO gap.[18] The largest gap follows the sequence: LER, ACR (*fa*-series), and TACR (*ta*-series), as shown in Table 6.

Objects of general formula $C_{N(k(56)^{k/2}(665)^{k/2})-Z[3k,n])}$ (like $C_{168(6(56)^3(665)^3)-Z[18,5])}$, Figure 1) represent properly closed shell fullerenes, the rule being a true LER, but written for zigzag cylinders, Z-LER: $N = 13k + 3km$; $k = 4, 6, 8, ...$; $m = 1, 2, ...$ The example in Figure 1 has a PC shell and shows a proper balance between a low HF and a high enough HOMO−LUMO gap (Table 2, entry 2). Note the wrong assessment[33] of this rule in a distinct zigzag cylinder rule or ZCR. For $k \neq 6$, the polar rings result by leapfrogging nontrivalent atoms in the parent cage.

The other PC structure in Table 2 is $C_{168(66^6(56)^6(65)^67^6(57)^3(75)^37^6)}$ (entry 6 and Figure 2); the azulenic ((5,7)3) covering, well-known being the aromatic conjugation in such systems,[34] appears as a stabilizing factor, even competing with the polyhex covering. The Stone−Wales[11] cascade edge rotation provides a route for isomerising between the polyhex (OP shell) and azulenic necks (PC shell) of the peanut structures (Table 2, entries 3−6). In the opposite, the intermediate $C_{168(66^6(56)^6(65)^67^656^4776^457^6)}$ (Table 2, entry 4) has a MC shell, suggesting a high kinetic instability. The peanut tubulenes in Figure 3 are PC cages (Table 5, entries 2 and 4). Such negatively curved cages, by the presence of rings larger than hexagons, have been observed by transmission electron microscopy or TEM, in the coalescence reactions[35] occurring in C_{60} peapods[36] (see below). Recall the involvement of such tessellations in the building of molecular structures of high genus.[37]

The OP class may be split in two subclasses: one with degenerate HOMO and LUMO orbitals in the positive domain of eigenvalues (the usual case; see Table 3, entries 2 and 4) and the other one with location in the negative domain (Table 2, entry 3). It appears that ((6,7)3) covering is responsible for the shift of HOMO eigenvalue in the negative domain (see also the MC cage, above).

In classical fullerenes (those having only pentagons and hexagons) no one MC shell example was reported so far; the OP shell in the negative domain appears in tetrahedral fullerenes only at $N = 628$.[31]

Note that the difference between the spectral gap and the semiempirical one may be explained by the rough approximation in simple Hückel theory that does not consider the σ orbitals.

Cages ((5,7)3) are unstable (see Table 3 and Table 4, entry 1) and tend to rearrange to the more stable *fa*-tubulenes (Table 4, entry 6 and Figure 12) by SW cascade edge rotations. The "blue" route appears more favored, as their HF values (Table 4, entries 2 and 3) are lower than those for the "red" route (Table 4, entries 4 and 5).

The POAV1 analysis shows that the positive curvature of the caps tends to flatten in the middle region of the *f*-tubulenes (Figure 1), the remaining strain (see Table 5) originating in the nanotube shape, of course more strained than the graphite sheet taken as reference. The peanut isomers (Figure 3 and Table 5, entries 2 and 4) are clearly more strained, even though the negative curvature in the middle

zone brings some strain relaxation. Their strain is, however, significantly lower than that calculated for twice C_{60} (8.257 kcal/mol), which roughly approximates the strain of the sp^3 [2 + 2] adduct.[20] These results are in agreement with the higher HF values compared to those for the *f*-tubulenes (Table 5).

The zeppelin-like cages (as those in Figures 1 and 13) were inferred[36,38] in coalescence reactions occurring in C_{60} peapods. A diameter increasing of the inner tube of a double-walled nanotube or DWNT, formed by heating peapods over 900 °C, was explained[38] by chirality changing (e.g., from (6,3)A to (6,3)Z tube, which further twisting increases its diameter—as previously proposed by us[39]), in the sense of minimization of the total energy of DWNT. Corrugated inner tubules appeared (e.g., having repeat units of peanut-shape, like the objects in Figure 3) by prolonging the peapods thermal annealing or by electron irradiation.[36]

Topology of ((5,7)3) periodic cages is satisfactory described by the tiling counting theorem (Table 1).

CONCLUSIONS

Various caps were used for capping nanotubes thus leading to finite cages, herein called tubulenes, related to the classical fullerenes. Such cages may show either a topological or both topological and electronic periodicity. Periodic cages with ((5,7)3) covering were illustrated and their constitutive typing enumeration were given.

Periodic cages with (6,3) covering in the distancing tube zone show electronic periodicity, in simple π-electron Hückel theory, as shown by several "rules of thumb". The π-electronic structure of the modeled cages showed a full pallet of shells with a clear relationship skeleton-electronic structure.

Some oligomers have a pretty low heat of formation. Peanut "dimers" were confirmed in experiments with C_{60} peapods.

REFERENCES AND NOTES

(1) Zorc, H.; Tolić, Lj. P.; Martinović, S.; Srzić, D. *Fullerene Sci. Technol.* **1994**, *2*, 471−480.
(2) Diedrich, F.; Thilgen, C. *Science* **1996**, *271*, 317−323.
(3) Neretin, I. S.; Lyssenko, K. A.; Antipin, M. Yu.; Slovokhotov, Yu. L.; Boltalina, O. V.; Troshin, P. A.; Lukonin, A. Yu.; Sidorov, L. N.; Taylor, R. *Angew. Chem. Int. Ed.* **2000**, *39*, 3273−3276.
(4) Qian, W.; Rubin, Y. *Angew. Chem. Int. Ed.* **2000**, *39*, 3133−3137.
(5) Lee, K.; Lee, Ch. H.; Song, H.; Park, J. T.; Chang, H. Y.; Choi, M.-G. *Angew. Chem. Int. Ed.* **2000**, *39*, 1801−1804.
(6) Fässler, T. F.; Hoffmann, R.; Hoffmann, S.; Wörle, M. *Angew. Chem. Int. Ed.* **2000**, *39*, 2091−2094.
(7) Zheng, J.-Y.; Noguchi, Sh.; Miyauchi, K.; Hamada, M.; Kinbara, K.; Saigo, K. *Fullerene Sci. Technol.* **2001**, *9*, 467−475.
(8) Mackay, A. L.; Terrones, H. *Nature* **1991**, *352*, 762.
(9) Gao, Y. D.; Herndon, W. C. *J. Am. Chem. Soc.* **1993**, *115*, 8459−8460
(10) Fowler, P. W.; Heine, T.; Manolopoulos, D. E.; Mitchell, D.; Orlandini, G.; Schmidt, R.; Seiferth, G.; Zerbetto, F. *J. Phys. Chem.* **1996**, *100*, 6984−6991.
(11) Stone, A. J.; Wales, D. J. *Chem. Phys. Lett.* **1986**, *128*, 501−503.
(12) Endo, M.; Kroto, H. W. *J. Phys. Chem.* **1992**, *96*, 6941−6944.
(13) Klein, D. J.; Zhu, H. All-conjugated carbon species. In *From Chemical Topology to Three—Dimensional Geometry*; Balaban, A. T., Ed.; Plenum Press: New York, 1997; pp 297−341.
(14) Diudea, M. V. *Bull. Stiint. Univ. Baia Mare Ser. B* **2002**, *18*, 31−38.
(15) Diudea, M. V. *Int. J. Nanosci.* **2003**, *2*, 171−183.
(16) Manolopoulos, D. E.; May, J. C.; Down, S. E. *Chem. Phys. Lett.* **1991**, *181*, 105−111.
(17) Hamada, N.; Sawada, S.; Oshiyama, A. *Phys. Rev. Lett.* **1992**, *68*, 1579−1581.
(18) Diudea, M. V. *Phys. Chem. Chem. Phys.* **2004**, *6*, 332−339.
(19) Diudea, M. V. *Fullerene Nanotub. Carbon Nanostruct.* **2002**, *10*, 273−292.
(20) Lebedkin, S.; Hull, W. E.; Soldatov, A.; Renker, B.; Kappes, M. M. *J. Phys. Chem. B* **2000**, *104*, 4101−4110.
(21) Dress, A.; Brinkmann, G. *MATCH, Commun. Math. Comput. Chem.* **1996**, *33*, 87−100.
(22) HyperChem, Release 4.5 for SGI, 1991−1995, HyperCube, Inc.
(23) Haddon, R. C. *J. Am. Chem. Soc.* **1990**, *112*, 3385−3389.
(24) Haddon, R. C.; Raghavachari, K. In: *Buckminsterfullerenes*; Billups, W. E., Ciufolini, M. A., Eds.; VCH: 1993; pp 185−215.
(25) Haddon, R. C.; Chow, S.-Y.*J. Am. Chem. Soc.* **1998**, *120*, 10494−10496.
(26) Haddon, R. C. *J. Phys. Chem. A* **2001**, *105*, 4164−4165.
(27) Ursu, O.; Diudea, M. V. TOPOCLUJ software package; "Babes-Bolyai" University, Cluj, 2003.
(28) Hückel, E. *Z. Phys.* **1931**, *70*, 204−286.
(29) Fowler, P. W.; Pisanski, T. *J. Chem. Soc., Faraday Trans.* **1994**, *90*, 2865−2871.
(30) Fowler, P. W.; Steer, J. I. *J. Chem. Soc., Chem. Commun.* **1987**, 1403−1405.
(31) Fowler, P. W. *J. Chem. Soc., Faraday Trans.* **1997**, *93*, 1−3.
(32) Fowler, P. W. *J. Chem. Soc., Faraday Trans.* **1990**, *86*, 2073−2077.
(33) Diudea, M. V. *Studia Univ.* "*Babes-Bolyai*" **2003**, *48*, 31−40.
(34) Kirby, E. C. *MATCH, Commun. Math. Comput. Chem.* **1996**, *33*, 147−156.
(35) Yeretzian, C.; Hansen, K.; Diedrich, F.; Whetten, R. L. *Nature* **1992**, *359*, 44−47; Aragón, J. L.; Terrones, H.; Romeu, D. *Phys. Rev. B* **1993**, *48*, 8409−8411.
(36) Hernández, E.; Meunier, V.; Smith, B. W.; Rurali, R.; Terrones, H.; Buongiorno Nardelli, M.; Terrones, M.; Luzzi, D. E.; Charlierr, J.-C. *Nano Lett.* **2003**, *3*, 1037−1042.
(37) Terrones, H.; Terrones, M. *Phys. Rev. B* **1997**, *55*, 9969; *Carbon* **1998**, *36*, 725−730;
(38) Bandow, S.; Hiraoka, T.; Yumura, T.; Hirahara, K.; Shinohara, H.; Iijima, S. *Chem. Phys. Lett.* **2004**, *384*, 320−325.
(39) Diudea, M. V.; Balaban, T. S.; Kirby, E. C.; Graovac, A. *Phys. Chem. Chem. Phys.* **2003**, *5*, 4210−4214.

CI049738G